

¹*Panpan Deng

Coordinated Control Strategy Based on Virtual Synchronous Generator Technology in New Energy System



Abstract: - The innovative system control strategy of chemical energy-based virtual synchronous generator technology combines the principles of energy storage and virtual synchronous generator techniques to achieve stable generation and transmission of electrical energy. With the increasing integration of new energy sources into the grid, the existing grid-connected inverters utilizing direct current control struggle to effectively regulate the load fluctuations of the grid. In this paper, a mathematical model is established that includes both the energy storage system and the integration of new energy sources. By integrating optimal coordination control theory with coordinated control regulations, a coordinated control regime is developed, including the design of a damping controller. Additionally, a control strategy based on communication delay is employed to ensure active involvement of the rectifier side of the direct current transmission line at the appropriate timing. Analysis reveals that as the power of the direct current transmission line increases, the coupling between the virtual synchronous generator and direct current transmission becomes stronger within specific frequency bands, which may lead to subsynchronous oscillations and result in system instability. Compared to traditional control strategies, the proposed chemical energy-based virtual synchronous generator technology presented in this paper effectively resolves the coupling challenges within specific frequency bands, suppresses subsynchronous oscillations, exhibits improved robustness, and allows the system to more flexibly respond to complex load fluctuations and new energy source fluctuations.

Keywords: Energy Storage, New Energy Grid, Virtual Synchronous Generator, Subsynchronous Oscillation, Coordinated Control.

I. INTRODUCTION

Amidst the dual-carbon landscape, the power system has been undergoing profound transformations in recent years. In the realm of addressing the energy crisis, the gradual substitution of traditional fossil fuels with clean and renewable energy sources has emerged as the sole alternative trajectory aligned with carbon peak and carbon neutral objectives. Seizing this opportunity, the installed capacity of photovoltaic, wind power, and other sources has experienced rapid growth.

The integration of new energy units into the grid involves a substantial number of power electronic components. Typically, photovoltaic and wind power generation units are linked to the power grid via constant current source converters based on phase-locked ring synchronization principles. However, these converters lack the physical response frequency modulation capability possessed by traditional synchronous generators with fixed rotors. Consequently, they exhibit weak damping characteristics and low inertia.

Moreover, new energy power generation connections are often situated far from load centers, in regions characterized by weak grid connections. As the scale of grid integration continues to expand, the substantial penetration of new energy sources into the power grid could potentially undermine the grid's capacity to manage power fluctuations. This scenario may even jeopardize the secure and stable operation of the entire system.

A energy storage system is a technology that can store energy in chemical form and release it when needed. In the realm of power systems, a energy storage system typically involves converting electrical energy into chemical energy, storing it within chemical reactions, and then converting it back into electrical energy for supply to the power grid when required. These energy storage systems serve various roles within power systems, such as load balancing, providing power reserves for peak demand, and offering backup power sources in the event of grid failures.

The Virtual Synchronous Generator (VSG) control strategy [1] is an active support approach. Based on synchronous current converter technology and inertial energy storage units, the VSG emulates the dynamic regulation behavior of synchronous generators in terms of active power frequency and reactive voltage. This furnishes the grid-connected inverters of renewable energy units with essential inertia and damping characteristics, addressing the inherent issues of low inertia and weak damping associated with these units. Reference [2] introduces an energy storage device for supporting primary energy output on DC busbars. Through VSG inverter control based on virtual inertial moment, the transient stability characteristics of the system can be dynamically

¹ Leshan Vocational and Technical College, Leshan, 614000, China

*Corresponding author: Panpan Deng

Copyright © JES 2024 on-line : journal.esrgroups.org

optimized. Reference [3] explores the bidirectional power control aspects of VSG. Reference [4] envisions the application of VSG in smart grids. A comprehensive review is conducted from the perspective of oscillation suppression during frequency, voltage, and inertia response processes, outlining the role of VSG in grid stability control and coordination.

The core concept of this study is to tightly integrate the energy storage system with the virtual synchronous generator control strategy, endowing it with a high degree of flexibility in energy management and regulation [5]. By simulating the active power support and frequency adjustment of synchronous generators, this approach contributes to the mechanistic analysis of coupled oscillations between the mechanical and electrical subsystems within the system [6]. Drawing on the pole placement technique from classical control theory and collaborating with the DC lines, a damping controller is designed. This controller is capable of effectively addressing load fluctuations or control disturbances within the system and adapting to the continuously changing operational conditions of the power grid.

II. ENERGY STORAGE SYSTEMS

A. AC/DC Hybrid Systems with Energy Storage

Energy storage systems represent an innovative approach to energy storage technology, offering superior charge-discharge conversion rates and overall system efficiency compared to traditional methods such as mechanical or thermal energy storage. At the core of a energy storage system are energy storage units, electrochemical reactions, and control and management systems. Fuel cells are employed as energy storage units, converting electrical energy to chemical energy during charging and converting it back during discharge. Electrochemical reactions form the foundation of energy storage, with different battery types or energy storage devices utilizing these reactions to store and release energy, their performance influenced by factors such as electrode materials, electrolytes, and temperature.

In the context of the system, photovoltaic power stations play a crucial role in supplying local loads and interfacing with the grid through high-voltage direct current (HVDC) connections via grid-connected inverters. energy storage systems are integrated into the photovoltaic power station's setup, employing multiple battery modules in series and then parallel arrangement to form battery packs. These systems are equipped with bidirectional converters, enabling high-capacity storage and rapid energy release over short durations. The management of charging and discharging relies on the active support control system of Virtual Synchronous Generator (VSG) [7], as depicted in Figure 1.

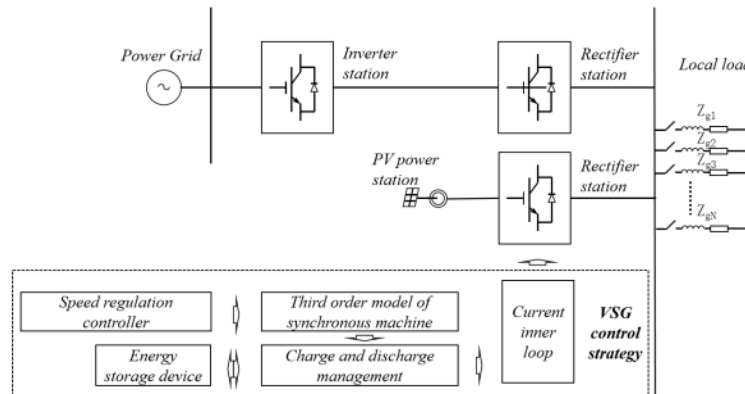


Figure 1: AC/DC Hybrid Systems with Energy Storage

B. The VSG Third-order Model

VSG is an advanced control strategy applied in power systems. Its core concept involves employing control strategies to emulate synchronous generator characteristics in non-synchronous new energy generators and energy storage systems. This includes emulating virtual mechanical inertia and voltage regulation capabilities. By continuously monitoring grid frequency and voltage in real-time and employing suitable control techniques, virtual synchronous technology enables rapid response to grid fluctuations and ensures the stability of power system frequency and voltage.

In this study, based on the system depicted in Figure 1, the third-order model of a synchronous machine is adopted to characterize the virtual synchronous generator. It consists of two main components: a speed regulation controller and an inertia damping model, which integrate the transient voltage regulation process of a synchronous

generator. The specific equations include the second-order rotor motion equation and the first-order transient voltage equation.

$$\begin{cases} \dot{\delta} = \omega - \omega_0 \\ \dot{\omega} = \frac{\omega_0}{H} (P_m - P_e) - \frac{D}{H} (\omega - \omega_0) \\ \dot{E}'_q = -\frac{1}{T_{d0}} E'_q + \frac{1}{T_{d0}} (x_d - x'_d) V_s \cos\delta + \frac{1}{T_{d0}} u_f \end{cases} \quad (1)$$

In the provided formula, several key variables are present: δ represents the power angle of the virtual generator, while ω signifies the angular speed. ω_0 denotes the rated angular speed, and D represents the damping coefficient. P_m stands for the mechanical power of the virtual generator, and P_e symbolizes the electromagnetic power of the virtual generator. The parameter H relates to the virtual inertia time. Furthermore, signifies the transient potential of the virtual synchronous motor, and E_{qe} pertains to the forced no-load electromomentum. T_{d0} represents the excitation winding time constant, while u_f signifies the input for the excitation control. The variables x_d and x'_d respectively represent the direct-axis synchronous resistance and the direct-axis instantaneous transformer resistance. Finally, V_s corresponds to the AC bus voltage.

The block diagram of the third order model of the synchronization machine is shown in Figure 2.

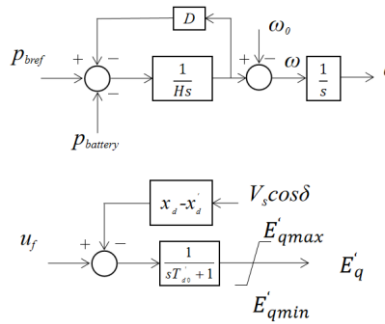


Figure 2: Standard Third-order Model of Synchronous Machine

C. Governor Design

VSG emulates the static frequency characteristics of a synchronous generator and achieves automatic unbalanced power adjustment [8] during system frequency modulation.

$$P_{bref} - P_{b0} = K_m (f_{meas} - f_{ref}) \quad (2)$$

In the equation: f_{ref} represents the frequency reference value, P_{bref} stands for the power reference value, and P_{b0} signifies the active power output of the energy storage system. f_{meas} denotes the measured value, while K_m denotes the Power-frequency ratio coefficient. During steady-state operation of the system, the PV generator operates in the Maximum Power Point Tracking (MPPT) mode. When influenced by external factors like sunlight or system disturbances, the speed regulation controller comes into play. It emulates the response of a synchronous generator's fixed rotor to changes in system frequency, adjusting power output and actively participating in power grid frequency modulation. To curb frequent charging and discharging of the energy storage device, a $\pm 0.03\text{Hz}$ dead zone is implemented based on testing. The governor's control diagram is illustrated in Figure 3.

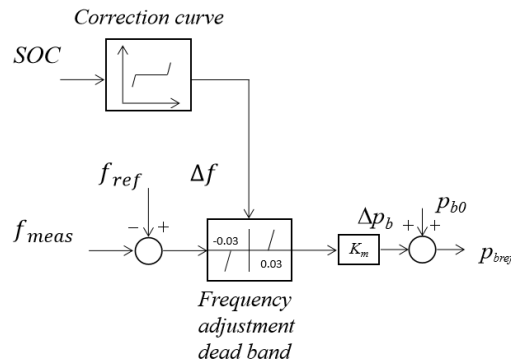


Figure 3: Governor Control Model

III. VSG CONTROL STRATEGY

The participation of VSG in power grid frequency adjustment unfolds in two distinct stages: the inertial response stage and the primary frequency adjustment stage. In the primary frequency adjustment stage, VSG

emulates the static frequency adjustment traits inherent in synchronous generators. A graphical representation of the relationship between the energy storage device and frequency variation when AC grid-side loads are switched on is depicted in Fig 4. Adhering to the frequency braking dead zone determined by the governor control model, the charge and discharge management system of the energy storage device opts to either remain locked or commence operation. When the frequency surpasses the dead zone range, the grid load disturbance and frequency alteration follow the set relationship curve. Within the same range of load fluctuations, notable reduction in steady-state frequency deviation of the power grid is achieved, allowing the system frequency to be maintained within a reasonable spectrum. Figure 4 illustrates that the contribution of VSG to system frequency adjustment in the primary frequency adjustment stage hinges upon factors such as the energy storage device's rated power, the rate of output power change, and the magnitude of rated power.

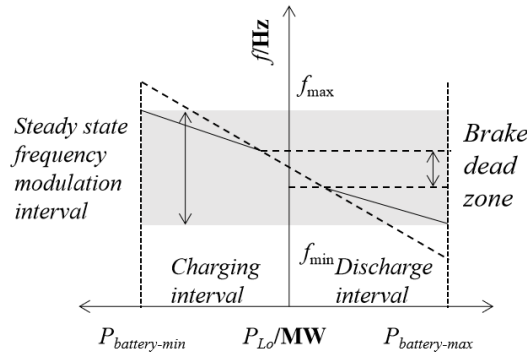


Figure 4: The Energy Storage Device Participates in the Primary Frequency Adjustment

IV. COORDINATED CONTROL STRATEGY BETWEEN VSG AND HVDC

A. Nonlinear System Linearization

Building upon the established VSG third-order model, and leveraging insights from classical control theory's pole movement approach, while also synergizing with DC lines [9], a resilient damping controller is formulated. This controller is designed to effectively manage load fluctuations and system disturbances within the system, while also flexibly adapting to the evolving operational dynamics of the power grid.

When investigating the stability control of an AC-DC system, the modulation of DC power can be perceived as a first-order inertial link.

$$\dot{P}_{dc} = \frac{1}{T_{dc}} (u_{dc} - P_{dc}) \quad (3)$$

u_{dc} represents the control input signal for DC power, while T_{dc} signifies the equivalent time constant of the DC system.

It's worth mentioning that the AC-DC hybrid connection system depicted in Figure 1.

$$P_e = P_L + P_{dc} \quad (4)$$

And the AC side load power is

$$P_L = \frac{E_q' V_S}{x_L} \sin \delta \quad (5)$$

x_L is reactance AC load-side.

By combining the equations (1), (3), (4), and (5) comprehensively, the entire system equation can be simplified as follows:

$$\begin{cases} \dot{\delta} = \omega - \omega_0 \\ \dot{\omega} = \frac{\omega_0}{H} P_m - \frac{D}{H} (\omega - \omega_0) - \frac{\omega_0}{H} (P_{dc} + \frac{E_q' V_S}{x_L} \sin \delta) \\ \dot{E}_q' = -\frac{1}{T_{d0}} E_q' + \frac{1}{T_{d0}} (x_d - x_d') V_s \cos \delta + \frac{1}{T_{d0}} u_f \\ \dot{P}_{dc} = \frac{1}{T_{dc}} (u_{dc} - P_{dc}) \end{cases} \quad (6)$$

In real-world systems, almost all systems exhibit some degree of nonlinear behavior, or the mathematical model of the entire system is described using nonlinear differential equations. Hence, in this section, the coordinated control system of the VSG and the HVDC will be accurately linearized using nonlinear control theory [10].

Based on the controller design objective, the outputs $y_1=h_1=\delta$, $y_2=h_2=P_{dc}$ are selected. The original system (6) constitutes a dual-input, dual-output system, and a dual-input, dual-output nonlinear system can be represented as:

$$\dot{x} = f(x) + g_1 u_1 + g_2 u_2$$

$$y = h(x)$$

$$x=(x_1,x_2,x_3,x_4)^T=(\delta,\omega,E_q',P_{dc})^T, g_1=(0,0,g_{11},0)^T=(0,0,1/T_{d0},0)^T, g_2=(0,0,0,g_{22})^T=(0,0,0,1/T_{dc})^T, y=(y_1,y_2)^T=(h_1,h_2)^T, u_1=u_f, u_2=u_{dc},$$

$$f(x) = [f_1(x)f_2(x)f_3(x)f_4(x)]^T = \begin{bmatrix} x_2 - \omega_0 \\ \frac{\omega_0}{H} P_m - \frac{D}{H} (x_2 - \omega_0) - \frac{\omega_0}{H} (x_4 + \frac{V_s x_3}{x_L} \sin x_1) \\ -\frac{1}{T_{d0}} x_3 + \frac{1}{T_{d0}} (x_d - x'_d) V_s \cos x_1 \\ -\frac{1}{T_{dc}} x_4 \end{bmatrix}$$

The nonlinear geometric linearization theory is applied to assess the degree of relationships within the system.

$$J(x) = \begin{pmatrix} b_{11} & b_{12} \\ b_{21} & b_{22} \end{pmatrix} \tag{7}$$

$$b_{11} = L_{g_1} L_f^2 h_1(x) = -g_{11} \frac{\omega_0 V_s}{H x_L} \sin x_1$$

$$b_{21} = L_{g_1} L_f^0 h_1(x) = 0$$

$$b_{12} = L_{g_2} L_f^2 h_1(x) = -g_{22} \frac{\omega_0}{H}$$

$$b_{22} = L_{g_2} L_f^0 h_1(x) = g_{22}$$

Obvious,

$$|J(x)| = -g_{11} g_{22} \frac{\omega_0 V_s}{H x_L} \sin x_1 \neq 0$$

The matrix $J(x)$ is nonsingular. With the set of relations degrees $r = \{r_1, r_2\} = \{3, 1\}$, the overall relationship degree of the system becomes $r = 3 + 1 = 4$. Consequently, for this scenario, the coordinate map $Z = \varphi(X)$ is chosen as follows:

$$z_1 = \varphi_1(x) = h_1(x) = x_1 \tag{8a}$$

$$z_2 = \varphi_2(x) = L_f h_1(x) = x_2 - \omega_0 \tag{8b}$$

$$z_3 = \varphi_3(x) = L_f^2 h_1(x) = f_2(x) \tag{8c}$$

$$z_4 = \psi_1(x) = h_2(x) = x_4 \tag{8d}$$

The multi-input and multi-output system satisfies the conditions for accurate linearization and can be transformed into the Brunovsky standard form [11].

$$\begin{cases} \dot{z}_1 = z_2 \\ \dot{z}_2 = z_3 \\ \dot{z}_3 = v_1 \\ \dot{z}_4 = v_2 \end{cases} \tag{9}$$

Where, $V = [v_1 v_2]^T$. Consequently, the coordinated control system of VSG and HVDC can be linearized as follows:

$$\dot{Z} = AZ + BV \tag{10a}$$

$$Y = CZ \tag{10b}$$

$$\text{Where } A = \begin{pmatrix} 0 & 1 & 0 & 0 \\ 0 & 0 & 1 & 0 \\ 0 & 0 & 0 & 0 \\ 0 & 0 & 0 & 0 \end{pmatrix} B = \begin{pmatrix} 0 & 0 \\ 0 & 0 \\ 1 & 0 \\ 0 & 1 \end{pmatrix} C = \begin{pmatrix} 1 & 0 & 0 & 0 \\ 0 & 0 & 0 & 1 \end{pmatrix}$$

State feedback is formulated using the chosen coordinate mapping relationship mentioned earlier:

$$\begin{bmatrix} u_1 \\ u_2 \end{bmatrix} = J^{-1}(x) \begin{bmatrix} v_1 - L_f^3 h_1(x) \\ v_2 - L_f^1 h_2(x) \end{bmatrix} \tag{11}$$

Where $L_1 = L_f^3 h_1(x) = k_1 x_3 \cos x_1 - k_2 x_2 x_3 \cos x_1 + k_3 x_2 + k_4 x_4 + k_5 x_3 \sin x_1 - k_6 \sin x_1 \cos x_1 + k_7$

$$L_2 = L_f^1 h_2(x) = -\frac{1}{T_{dc}} x_4$$

$$\begin{aligned}
 k_1 &= \frac{\omega_0^2 V_S}{H x_L} k_2 = \frac{\omega_0 V_S}{H x_L} k_3 = \frac{D^2}{H^2} \\
 k_4 &= \frac{\omega_0 D}{H^2} + \frac{\omega_0}{HT_{dc}} k_5 = \frac{\omega_0 D V_S}{H^2 x_L} + \frac{\omega_0 V_S}{T_{do} H x_L} \\
 k_6 &= \frac{(x_d - x'_d) \omega_0 V_S^2}{T_{do} H x_L} k_7 = \frac{\omega_0 D}{H^2} (P_m + D)
 \end{aligned}$$

General (7) and L_1, L_2 in substitution (11), the control law of the state feedback of the original nonlinear system is

$$\begin{bmatrix} u_1 \\ u_2 \end{bmatrix} = \begin{bmatrix} 1/b_{11}(v_1 - L_1) - k_{10}(v_2 - L_2) \\ 1/b_{22}(v_2 - L_2) \end{bmatrix} \tag{12}$$

Where $k_{10} = \frac{x_L}{g_{11} V_S \sin x_1}$

B. Optimal Coordination Controller Structure Design

Optimal control constitutes a significant field within modern control theory. The research problem within optimal control theory [12] can be succinctly framed as follows: Given a controlled dynamic system or a motion process, the objective is to determine an optimal control scheme from a set of permissible control strategies. This optimal control scheme guides the system's movement from an initial state to a desired target state while adhering to specific constraints. The aim is to calculate an optimal control law that enhances the performance index of the entire system.

Applying optimal coordination control theory to address the output feedback control law of a coordinated control system involves several steps. Initially, the subsystem controllers are formulated in a centralized manner.

$$U = K_d Y \tag{13}$$

Where $U = [u_1, u_2, \dots, u_N]^T$, $Y = [y_1, y_2, \dots, y_N]^T$. Define Ω as the set of partitioned diagonal matrices with K_d structural form. The problem that output feedback control is trying to solve: find a K_d that can minimize the quadratic performance index of the whole system.

$$J = \int_0^\infty [X^T(t) Q X(t) + U^T(t) R U(t)] dt \tag{14}$$

$Q \in R^{n \times n}$ is a positive semidefinite matrix. $R \in R^{r \times r}$ is a positive definite matrix.

A necessary condition for J to be minimized is the existence of a matrix group (P, V, K_d) satisfies the following *Levine-Athans* equations:

$$\begin{cases} P(A + BK_d C) + (A + BK_d C)^T P + Q + C^T K_d^T R K_d C = 0 \\ V(A + BK_d C) + V(A + BK_d C)^T + I = 0 \\ RK_d (CVC^T)_d + (B^T PVC^T)_d = 0 \end{cases} \tag{15}$$

In accordance with the principles of optimal coordination control design theory, the structure of the coordination controller is established as follows:

$$V = \begin{bmatrix} k_1 \\ k_2 \end{bmatrix} Y \tag{16}$$

Then the feedback gains k_1 and k_2 can be obtained according to the optimal coordinated control algorithm.

Finally, the obtained $V = K_d^* Y$ is substituted into equation (12) to obtain the coordinated control law of VSG and HVDC. Following the design concept of DC supplementary control as described in the Electric Power Research Institute (EPRI) report [13], this study opts to implement additional controllers on both the virtual synchronous generator side and the rectifier side of the DC transmission line.

C. Comprehensive Control of the Energy Storage Systems

In the autonomous power system based on the synchronization mechanism, the underlying control strategy is autonomously carried out by the charge and discharge of the energy storage system, independently of communication system control. The energy storage system exhibits fast response speed, which contributes to enhancing the reliability and safety of the system when facing minor disturbances. Moreover, when the system load undergoes significant changes, the different control parameters of power electronic components on each side can lead to varying dynamic response speeds, resulting in rapid dynamic responses and fast power generation. This phenomenon causes instantaneous fluctuations in the output frequency. If the system's dynamic performance

continues to deteriorate, the virtual synchronous generator control strategy might not offer sufficiently large dynamic damping adjustments. Therefore, for stability, it's necessary to manage the State of Charge (SOC) of the energy storage system and coordinate control strategies to maintain the SOC within a reasonable range.

By continuously monitoring the variations in the power grid's frequency and the SOC value of the energy storage system, the state quantity signals are established as depicted in equations (17) to (19), shown below.

$$T_1 = \begin{cases} 1, |\Delta f| \leq \Delta f_{set} \\ 0, |\Delta f| > \Delta f_{set} \end{cases} \quad (17)$$

$$T_2 = \begin{cases} 1, Q_{SOC} \in [0, Q_{SOCmin}] \\ 0, Q_{SOC} \in [Q_{SOCmin}, Q_{SOCmax}] \\ 1, Q_{SOC} \in [Q_{SOCmax}, 1] \end{cases} \quad (18)$$

$$T = T_1 \& T_2 \quad (19)$$

Where, T_1 is the frequency deviation state quantity signal, Δf_{set} is the frequency deviation allowable value, the mean is continuously sampled for the current 0.1s time of the system, T_2 is the charge state quantity signal of the energy storage device, Q_{SOCmin} , Q_{SOCmax} are the upper and lower limit warning values of the charge and discharge characteristics of the energy storage device, and T is the integrated control strategy signal.

Table 1: Integrated Control Execution Logic

T price	T ₁ price	T ₂ price	VSG control	Coordination Control
1	1	1	Recover	Shutting
0	0	0	Touch Off	Touch Off
	1	0	Touch Off	Shutting
	0	1	Delay Recovery	Touch Off

Based on Table 1, when T is set to 1, the VSG control strategy is activated to restore the SOC charge and discharge to the initial setting value. The coordination control strategy remains locked to maintain system stability, avoiding excessive control parameters and feedback during its operation. When T is set to 0, there are three cases to consider. If both T_1 and T_2 are set to 0, both the VSG control strategy and the coordination control strategy are triggered. The coordination control strategy actively enhances the system's dynamic response performance, bringing the system back to a steady state. If T_1 is set to 1 and T_2 is set to 0, the VSG control strategy is triggered while the coordination control strategy is locked. This allows the VSG control strategy to address minor load disturbances and changes in photovoltaic power output. On the other hand, if T_1 is set to 0 and T_2 is set to 1, the system is in an extreme operational state. This triggers the coordinated control strategy and surpasses the QSOC min limit value. HVDC and VSG work together to quickly restore the system to a stable state. When T is set to 1, the SOC charge and discharge return to the initial setting value promptly.

Consideration of communication latency is crucial when implementing a coordinated control strategy. The coordination control approach proposed in this paper relies on the interaction of information between the VSG and HDVC, and the transmission lag aligns more closely with real communication systems. Furthermore, the coordination control strategy involves minimal data transmission, boasts a brief communication span, and theoretically exhibits delays on the order of milliseconds.

Moreover, this strategy also mitigates instances where minor disturbances or harmonic triggers lead to frequent system starts and stops. Such scenarios can result in excessive adjustments to control parameters and irregular feedback loops, ultimately jeopardizing the stability of the power grid. Consequently, the proposed communication delay coordination control strategy aims to address the insufficiency of VSG's frequency modulation for maintaining system stability. By enhancing the system's dynamic response performance through coordinated control, transient response times are shortened. Simultaneously, this approach effectively curtails an overload of control parameters and feedback, ensuring excellent control performance across various conditions within the entire system.

V. SEMI-PHYSICAL REAL-TIME SIMULATION

A. Parameter Design

In order to demonstrate the effectiveness of the proposed control strategy for the energy storage system in regulating system frequency under continuous load fluctuations, this study established a real-time simulation platform based on Matlab/Simulink. The example structure of the platform is depicted in Figure 1. Using Matlab software, the mathematical model of the energy storage system was developed, and a communication module was

built for the VSG control strategy and rectifier station control. Networking was achieved through network cards and switches, and UDP protocol communication code was written to simulate remote information exchange.

The rectification side of the DC system employed constant current regulation, while the inverter side employed constant voltage regulation. Specific real-time simulation parameters are presented in the table, with the primary simulation parameters listed in Table 2.

B. Analysis of Traditional Control Strategies

To assess the efficacy of the VSG control strategy, real-time simulation scenarios as outlined in Table 3 were established. These scenarios were designed to examine the impact of variations in DC transmission power on the damping characteristics of the virtual synchronous machine. While keeping the parameters of the other system components constant, the DC power was set to values of P=0.6pu, 0.8pu, and 1.0pu. The outcomes in terms of active power output and the state of charge of the AC bus line are illustrated in Figure 5 and 6.

Table 2: The Main Parameters of Real-time Simulation

Communication frequency f / kHz	1
VSG Inertia of Turn J (kg/m ²)	2
VSG active activity coefficient K_0 (rad/MW)	4
VSG power rating P_0 /MW	4
Mutual damping D_m (N·ms/rad)	50
HVDC equivalent time constant T_{dc} /s	0.02
Energy storage and discharge early warning lower limit Q_{SOCmin}	20%
Energy storage and charging early warning upper limit Q_{SOCmax}	80%
Frequency deviation allowed value Δf_{set}	0.05Hz

Table 3: Real-time Simulation Working Condition Setting I

time /s	system mode	Input load / MW	Cut out load / MW
[0,1.5)	Interconnection	4	-

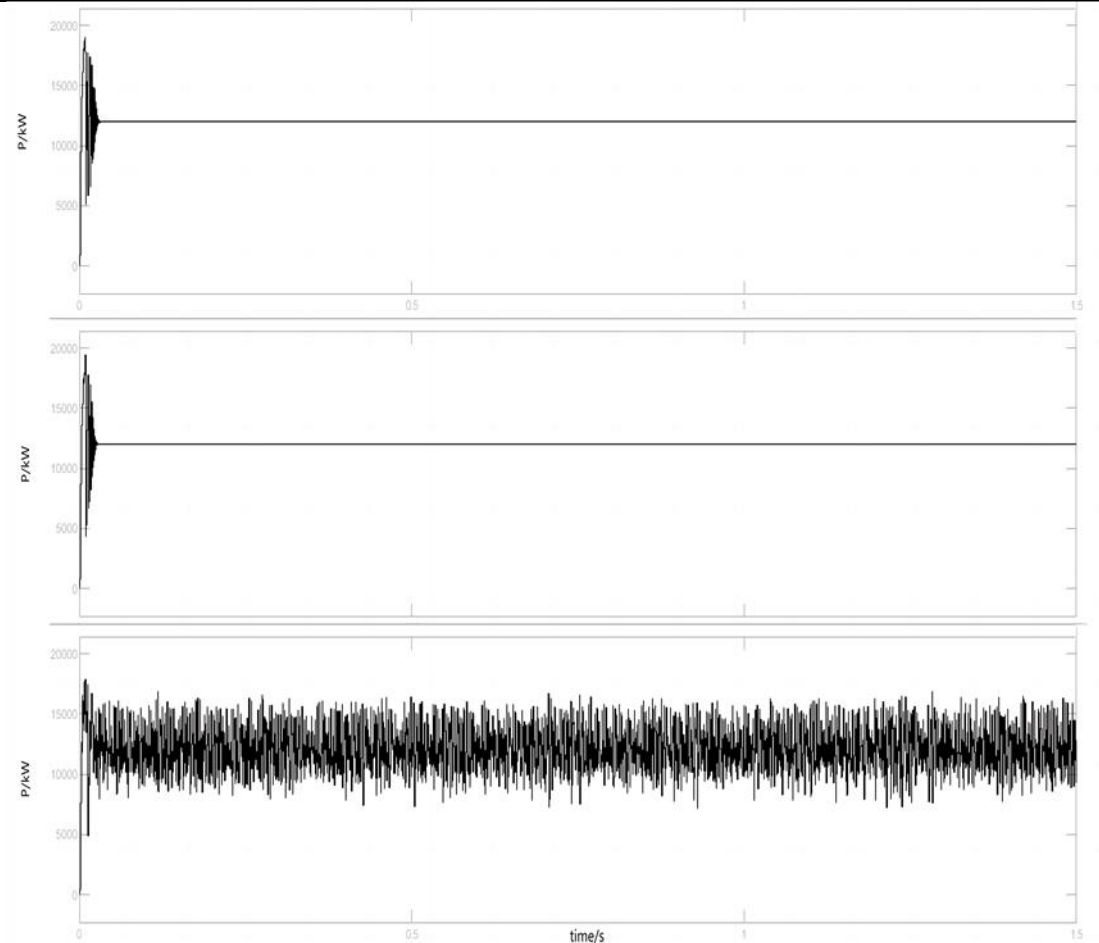


Figure 5: Power Waveform under VSG Control Strategy - Simulation Condition I

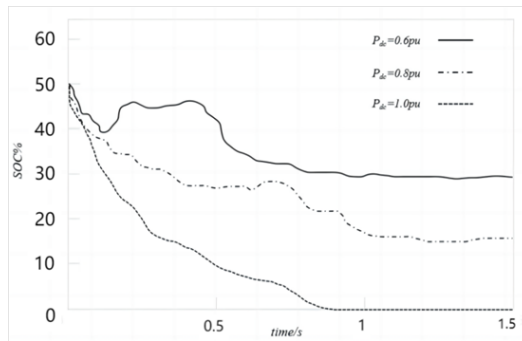


Figure 6: SOC Output Curve - Simulation Condition I

In the real-time simulation scenario labeled as Condition I, with DC power levels set at $P=0.6pu$ and $0.8pu$ at $t=0s$, the system is initially connected to the grid. Amid the interplay of input from impact loads and power startups, the presence of numerous power electronic components becomes evident. After a period of $0.2s$, the system attains power stability, maintaining a frequency of $50Hz$, while the energy storage device remains in a state of discharge. Post this transient adjustment, the system manages to uphold a steady power output. At a DC power level of $P=0.8pu$, the state of charge (SOC) of the energy storage device is just under 20% . At $P=1.0pu$, the figure reveals that due to the influence of the impact load, the active power within the system connection fails to stabilize, leading to enhanced oscillations and a noticeable sub-synchronous oscillation phenomenon. The SOC output curve corroborates that this phenomenon stems from the continuous output of the energy storage device exceeding its rated power limit.

The ability of the energy storage system to provide sufficient damping support largely depends on the virtual inertia and damping coefficient [14]. To further analyze the impact of the damping coefficient, a test signal method is employed to modify the established mathematical model by changing the power transmission capacity of the DC transmission line to obtain the electrical damping coefficient as depicted in Figure 7's characteristic curve. In this figure, when $P_{dc}=1.0pu$ and the frequency is $20Hz$, the system exhibits significant negative damping, leading to poor stability. Introducing the VSG control strategy at $P_{dc}=0.8pu$ while considering the perigee load Z_g significantly improves the system's damping characteristics. However, at a frequency of $15Hz$, the system still shows a negative damping trend, posing the risk of subsynchronous oscillations when disturbed. For $P_{dc}=0.6pu$, the AC-DC hybrid system is practically in a weakly coupled state, where the output of VSG predominates [15]. This state significantly enhances the system's damping characteristics, presenting negative damping only in the low-frequency band below $5Hz$.

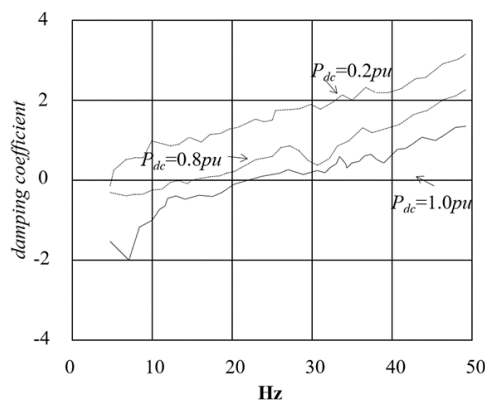


Figure 7: Electric Damping Coefficient Decharacteristic Curve

Based on the analysis results, the electrical damping coefficient exhibits significant negative values only below $20Hz$. The bandwidth of the HVDC rectifier-side fixed current controller typically falls below $20Hz$. This observation suggests that at $P_{dc}=1.0pu$, there exists a strong coupling between the Virtual Synchronous Generator (VSG) and the HVDC. Disturbances occurring within the $20Hz$ frequency range due to HVDC control will induce negative damping effects throughout the closed-loop system. In situations where the VSG control strategy fails to offer adequately substantial dynamic damping regulation [16], the system becomes destabilized, leading to sub-synchronous oscillations. When the DC system power level is brought down to $P_{dc}=0.6pu$ or $0.8pu$, the VSG control strategy can seamlessly transition into steady-state operation, drawing from its inherent inertia. This smooth transition ensures system stability.

C. Coordinate the Control Strategy Analysis

To validate the efficacy of the coordination control strategy grounded in VSG control, a real-time simulation scenario depicted in Table 3-4 is established, with the DC power set at $P_{dc}=1.0pu$. The outcomes are displayed in Figure 8 to 10.

Table 4: Sequences of Real-time Simulation II

Time /s	System mode	Input load / MW	Cut out load / MW
0	Interconnection	4	-
[0.5,1)	-	2	-
[1,1.5)	-	-	4

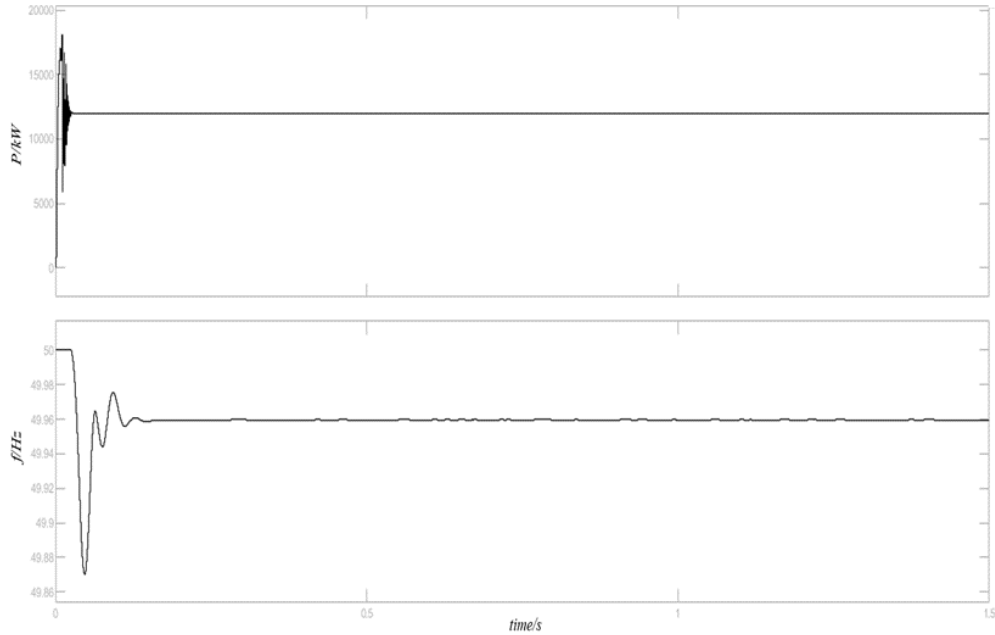


Figure 8: Power and Frequency Waveform under Coordinated Control Strategy - Simulation Condition I

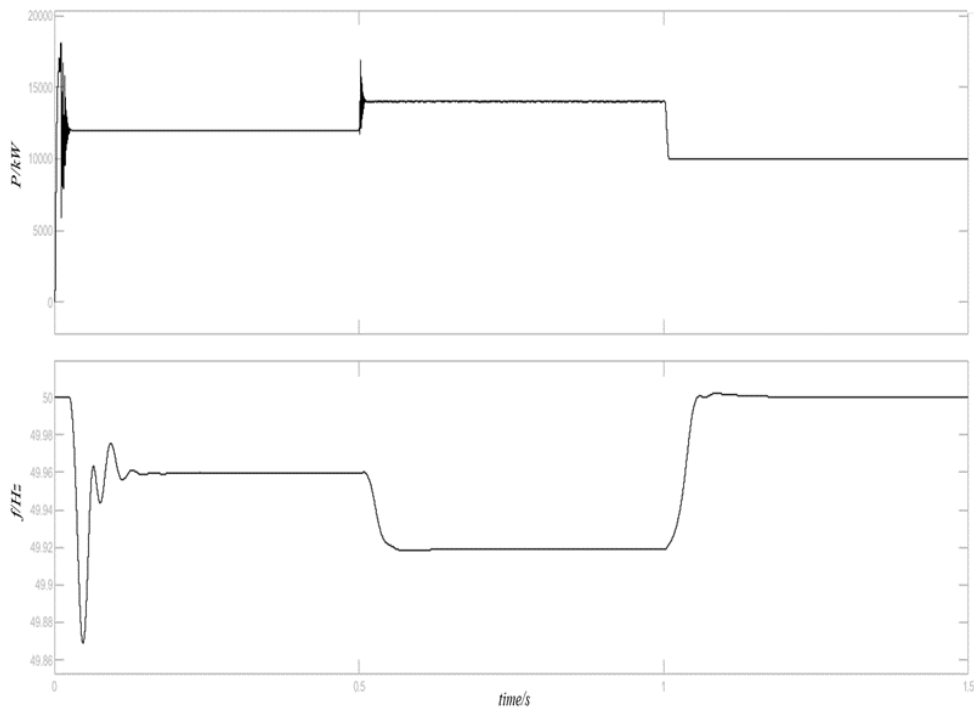


Figure 9: Power and Frequency Waveform under Coordinated Control Strategy - Simulation Condition II

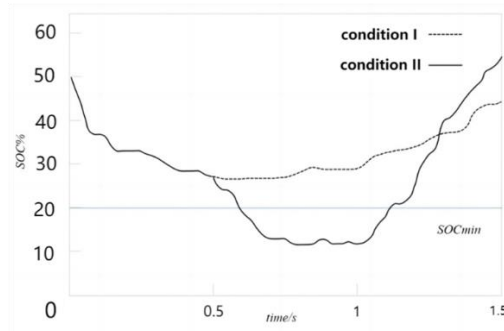


Figure 10: SOC Output Curve - Simulation Condition I/II

Based on the simulation conditions presented in Fig 8, the system starts grid connection at $t=0$ seconds. Under the influence of a significant impact load, the active power at the connection point stabilizes after a brief oscillation. The coordination control strategy effectively suppresses active power oscillation [17], ensuring stable system frequency. Fig 10 illustrates that the SOC curve of the energy storage system experiences no overcharging or over-discharging. At $t=0.5$ seconds, the SOC of the energy storage system begins to charge, confirming the effectiveness of the integrated control execution logic setting.

The response of the system under continuous load changes can be observed from simulation condition II in Fig 9. After introducing a 4MW impact load, the active power at the connection point stabilizes after a short oscillation. At $t=0.5$ seconds, a 2MW impact load is applied, and the system tends to stabilize after a brief power oscillation. It's evident that the coordinated control strategy effectively suppresses oscillation following delayed communication initiation. When a 4MW impact load is disconnected at $t=1$ second, the system's connected power smoothly decreases to near the rated value, primarily regulated by the VSG control strategy. It's apparent that the integrated control execution logic setting in the coordination control strategy is effective. As shown in Fig 10, the SOC curve of the energy storage system reaches the lower discharge warning limit of $Q_{SOCmin}=20\%$ around $t=0.6$ seconds, and the comprehensive control logic continues to execute [18]. The system tends to stabilize around $t=0.7$ seconds, and the system initiates charging back at $t=1$ second to balance power output.

Simulation results reveal that for localized small-load disturbances, the VSG control strategy can promptly achieve the target of suppressing connected power. Due to the configuration of energy storage system capacity and its own rotational inertia and damping characteristics, relying solely on the VSG control strategy is insufficient to suppress large-load disturbances beyond the bearing capacity [19]. Interaction among power electronic components can lead to subsynchronous oscillation. However, the coordinated control strategy is capable of effectively handling continuous load changes, suppressing connected power oscillation, and achieving a more robust system without the need for additional energy storage capacity.

VI. CONCLUSIONS

This paper addresses the issue of power oscillation resulting from the limited self-adjustment capability of new energy systems. It proposes a VSG control strategy based on energy storage systems, and further employs a coordination control strategy based on communication delay [20]. This coordination strategy involves designing a damping controller to work in conjunction with the virtual synchronous generator, providing active support control. Research findings indicate that the active support control strategy based on energy storage VSG provides excitation and speed regulation characteristics similar to a synchronous generator. This significantly enhances the system's frequency regulation and voltage stabilization capabilities. Changes in the power of the DC transmission line influence the electrical damping coefficient. Properly configuring the capacity and parameters of the energy storage system ensures stable dynamic response and damping characteristics under different power variation scenarios. The coordination control strategy, based on communication delay and incorporating a damping controller, addresses evolving system operational conditions. This approach is particularly effective for systems with strong coupling between VSG and HVDC on the HVDC rectifier side bandwidth. When it comes to DC additional damping control, transitioning from a single-frequency target control to an integrated control of frequency and power enhances the system's dynamic performance.

This study has not extensively investigated additional potential issues and challenges within the new energy system, such as those related to grid scalability and reliability. In-depth exploration of the potential of coordination control strategies will be the focal point of future research endeavors. This will entail meticulous parameter refinement and optimization through methodologies including simulation and emulation, aimed at bolstering the system's stability and robustness.

ACKNOWLEDGMENTS

Foundation Project: Supported by Science and Technology Project of Leshan City (No.22ZDYJ0153).

REFERENCES

- [1] Han Feng, Zhang Xing, Guo Zixuan, Wang Jilei, Fu Xinxin, Gao Bo. A comparative study of single-loop VSG and multi-loop VSG. *Energy Reports*, 2022, 8(S5).
- [2] He Guofeng, Zhao Le, Dong Yanfei, Li Guojiao, Zhang Wenjie. A Novel VSG Control Strategy for UPS Voltage Source Inverter with Impulsive Load. *Energies*, 2022, 15(13).
- [3] Karanveer Dhingra, Mukesh Singh. Smart Charging Station to Cater the Sudden Ingress and Egress of EVs while Supporting the Frequency of Microgrid through VSG. *Arabian Journal for Science and Engineering*, 2020, 45(8).
- [4] Mohd Hanif Othman, Hazlie Mokhlis, Marizan Mubin, Saifal Talpur, Nur Fadilah Ab Aziz, Mohamad Dradi, Hasmaini Mohamad. Progress in control and coordination of energy storage system-based VSG: a review. *IET Renewable Power Generation*, 2020, 14(2).
- [5] Fang Jianfeng, Zhao Jinbin, Mao Ling, Qu Keqing, Gao Zixuan. An improved virtual synchronous generator power control strategy considering time-varying characteristics of SOC. *International Journal of Electrical Power and Energy Systems*, 2023, 144.
- [6] Tian Xinshou, Chi Yongning, Li Yan, Tang Haiyan, Liu Chao, Su Yuanyuan. Sub-synchronous oscillation coordinated damping optimization control of DFIG and VSG and self-optimization parameter tuning method. *CSEE Journal of Power and Energy Systems*, 2019, 7(1).
- [7] Mohamed Mahmoud M., El Zoghby Helmy M., Sharaf Soliman M., Mosa Magdi A. Optimal virtual synchronous generator control of battery/supercapacitor hybrid energy storage system for frequency response enhancement of photovoltaic/diesel microgrid. *Journal of Energy Storage*, 2022, 51.
- [8] J. Descusse, Michel Fliess, A.Isidori, D.Leborgne. *New Trends in Nonlinear Control Theory*. Springer Berlin Heidelberg. Springer, Berlin, Heidelberg: 2006-01-01.
- [9] Seyed Kamaledin Yadavar Nikravesh. *Nonlinear Systems Stability Analysis: Lyapunov-Based Approach*. CRC Press: 2018-09-03.
- [10] Leonard David Berkovitz, Negash G.Medhin. *Nonlinear Optimal Control Theory*. Taylor and Francis. CRC Press: 2012-08-28.
- [11] Richard J P, Einar V L. HVDC System Control for Damping of Subsynchronous Oscillations. *IEEE Transactions on Power Apparatus and Systems*, 1982, 101(7): 2203-2211.
- [12] Zheng Tianwen, Chen Laijun, Guo Yan, Wei Wei, Zhou Bo, Sun Xinwei. A VSG-Based Coordinated DC Voltage Control for VSC-HVDC to Participate in Frequency Regulation. *Energies*, 2021, 14(9).
- [13] Huadian Xu, Jianhui Su, Ning Liu, Yong Shi. A Grid-Supporting Photovoltaic System Implemented by a VSG with Energy Storage. *Energies*, 2018, 11(11).
- [14] Yong, Shi. Inertia Parameter Selection Method for HVDC Converter Station Based on VSG Control. *Journal of Electrical Engineering & Technology*. Prepublish (2021).
- [15] Liang Yalin, He Yuyao, Niu Yun. Microgrid Frequency Fluctuation Attenuation Using Improved Fuzzy Adaptive Damping-Based VSG Considering Dynamics and Allowable Deviation. *Energies*, 2020, 13(18).
- [16] Liu, H. Chen, Z. Contribution of VSC-HVDC to Frequency Regulation of Power Systems with Offshore Wind Generation. *IEEE Trans. Energy Convers.* 2015, 30, 918-926.
- [17] Tiziano D,Salvatore S,Chiara A T, et al. Performance of an Indirect Packed Bed Reactor for energy storage. *Materials*, 2021, 14(18).
- [18] Robert S. energy storage enables the transformation of fossil energy systems to sustainability. *GREEN CHEMISTRY*, 2021, 23(4).
- [19] Energy; New Findings from ITMO University Describe Advances in Energy (Introducing a Hybrid Mechanical - energy storage System: Process Development and Energy/exergy Analysis). *Energy & Ecology*, 2020.
- [20] Chi Y,Shuanshi F,Xuemei L, et al. Hydrogen and energy storage in gas hydrate at mild conditions. *International Journal of Hydrogen Energy*, 2020, 45(29).